

# Detection of Temporal Changes in Vegetative Cover on South Padre Island, Texas Using Image Classifications Derived from Aerial Color-Infrared Photographs

Rubén A. Mazariegos<sup>1,\*</sup>, Kenneth R. Summy<sup>1</sup>, Frank W. Judd<sup>1</sup>,  
Robert I. Lonard<sup>1</sup>, and James H. Everitt<sup>2</sup>

<sup>1</sup>The University of Texas Rio Grande Valley, 1201 W. University Dr., Edinburg, TX 78539

<sup>2</sup>Agricultural Research Service, U. S. Department of Agriculture (retired)

\* Corresponding author: ruben.mazariegos@utrgv.edu

## ABSTRACT

Supervised image classifications developed from 23 x 23 cm aerial color-infrared aerial photographs (1:5,000 scale) were used to evaluate temporal changes in vegetative cover occurring within three 150 x 300-m research sites on South Padre Island, Texas. Use of high-resolution digitized imagery (ground pixel resolution of ca. 0.1 m) and survey-grade GPS for positional measurements of ground control points (20-25 1.0m<sup>2</sup> targets within each research site) resulted in consistently high levels of geometric accuracy, with root mean square errors (RMSEs) ranging between 0.397 – 2.867. Similarly, use of relatively simple information categories (dry and wet sand, live and dead vegetative cover, and water) resulted in supervised image classifications with consistently high levels of overall thematic accuracy (90.0 – 98.0%). Temporal comparisons of image classifications using a cross-tabulation procedure indicated that changes in total vegetative cover had been minimal at most locations during the course the two-year study (2003-2005). However, a localized but significant disruption of native vegetation caused by the dumping of sand by highway maintenance crews was detected in one of the study sites (2004), and ground inspection revealed numerous other sand-dumping sites at various locations on the barrier island. In the first situation, comparison of CIR aerial photographs acquired before and after the sand-dumping incident provided a reliable means by which to evaluate the extent of damage caused by the dumped sand, and to monitor its eventual recovery as a result of recolonization by native plant species.

*Additional index words:* : Remote sensing, aerial photography, image analysis, image classification, coastal vegetation.

Because of its importance in the stabilization of dune systems and other coastal landscape features, the native vegetation of South Padre Island has been studied intensively during the past thirty years (Judd et al. 1977, 2007, 2008; Lonard and Judd 1980, 1981, 1997; Lonard et al. 1978; 1999; Richardson 2002). In addition to documenting the seasonal abundance and spatial distribution of various plant species, studies of coastal vegetation have documented the effects of sporadic events such as major freezes and damage caused by tropical storms and hurricanes (Judd and Sides 1983; Lonard and Judd 1985, 1991, 1993). Many of the latter studies have been facilitated by the use of remote sensing technology, including aerial color-infrared (CIR) photography, multispectral videography and hyperspectral imagery acquired from aircraft platforms (Everitt and Judd 1989; Everitt et al. 1991,

1996, 2007). More recently, the effectiveness of high-resolution sensors onboard commercial satellites, e.g., Quickbird (DigitalGlobe, Inc., Longmont, CO) for identifying and monitoring coastal vegetation in southern Texas has been demonstrated (Everitt et al. 2008).

One of the most common uses of multispectral and hyperspectral imagery (characterized by several to many waveband images, respectively) is the development of thematic maps from various types of automated image classifications (Lillesand et al. 2004; Jensen 2005; Campbell 2007). Essentially, image-processing software is designed to identify “natural spectral classes” in imagery with little or no input from the image analyst (unsupervised classifications) or to classify imagery into meaningful information classes using “training” data (pixel samples with known identity) provided by the analyst (supervised classifications).

In cases in which certain important landscape features represent a mixture of two or more categories (e.g., wetlands, which include both vegetation and water), image classifications are commonly based on the use of “fuzzy logic” which classifies image pixels according to the percentage contribution of each category (Lillesand et al. 2004; Jensen 2005; Campbell 2007).

Image classifications or thematic maps developed from imagery acquired on two or more dates are commonly compared to assess temporal changes in various landscape features during known time intervals (Lunetta and Elvidge 1999; Jensen 2005). One major advantage of using image classifications rather than raw imagery in such comparisons is that the former are directly comparable over a series of dates whereas the latter may require normalization (radiometric corrections) before temporal comparisons are made (Jensen 2005). However, since multitemporal comparisons of thematic maps are generally made on a pixel-by-pixel basis, a sufficiently high degree of geometric and thematic accuracy is critical for obtaining meaningful results in such change-detection analyses (Congalton and Green 1999).

In an effort to evaluate temporal changes in vegetative cover within dune fields on South Padre Island, we conducted a two-year study (2003-2005) in cooperation with the Coastal Management Program of the Texas General Land Office. Specific objectives of the project included the following: 1) evaluate the spectral properties of common plant species and other landscape features (e.g., residue of dead vegetation, dry and wet sand, and water) occurring within selected dune fields, 2) acquire and process aerial color-infrared (CIR) photographs of research sites at selected time intervals, 3) develop image classifications from aerial CIR photographs and assess their geometric and thematic accuracy, and 4) compare image classifications for each site to evaluate the magnitude of temporal changes in vegetative cover occurring during each time period (Summy et al. 2005a, 2005b; Judd et al. 2007, 2008).

## MATERIALS AND METHOD

**Description of Research Sites.** Three research sites, each measuring ca.  $150 \times 300$  m, were established along a 10-km segment of Hwy 100 on South Padre Island (Figure 1a). The first of these was located within an undisturbed “dune protection zone” (southern boundary coordinates from  $26^{\circ} 8' 35.67''$  N,  $97^{\circ} 10' 19.2''$  W to  $26^{\circ} 8' 36.5''$  N,  $97^{\circ} 10' 8.76''$  W), in which native vegetation was relatively abundant and diverse (Figure 1b). A second site, located 5 km north of the first (southern boundary coordinates

from  $26^{\circ} 11' 9.6''$  N,  $97^{\circ} 10' 35.4''$  W to  $26^{\circ} 11' 9.6''$  N,  $97^{\circ} 10' 29.28''$  W), had been disturbed by to a considerable extent as a result of human activities (primarily foot and vehicular traffic), although a considerable amount of native vegetation was still present (Figure 1c). A third site, located near the north end of Highway 100 (southern boundary coordinates from  $26^{\circ} 14' 34.26''$  N,  $97^{\circ} 11' 8.16''$  W to  $26^{\circ} 14' 34.188''$  N,  $97^{\circ} 11' 1.32''$  W), had been disrupted by human activities to such an extent that native vegetation and plant residue was essentially absent (Figure 1d). Species abundance and richness within each of these sites was summarized by Judd et al. (2008).

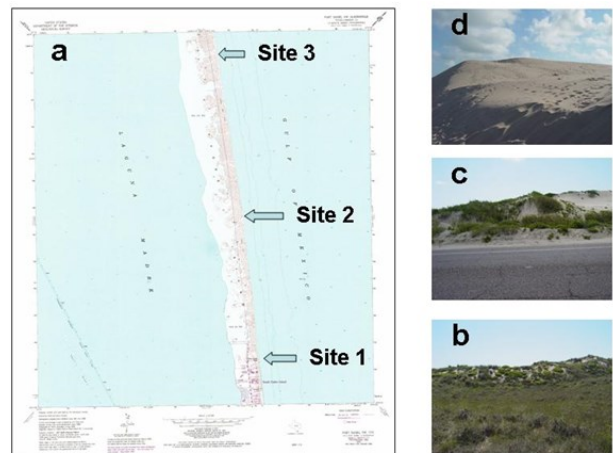


**Fig. 1.** USGS South Padre Island Quadrangle Map showing locations of the three research sites (a) and ground-level photographs of primary dune areas in Site 1 (b), Site 2 (c) and Site 3 (d).

**Spectral Reflectance Measurements.** Spectral reflectance measurements of dominant native plant species, dead standing vegetation, wet and dry sand and other landscape features of interest (Figures 2 and 3) were measured in situ using a FieldSpec<sup>®</sup> Dual VNIR spectroradiometer (Analytical Spectral Devices, Inc., Boulder, CO). This instrument is designed to measure electromagnetic radiation (EMR) extending from the ultraviolet (350 – 400 nm) through the near-infrared regions of the spectrum (700 – 1100 nm) in 10-nm increments, and is normally used with both a target sensor for measuring EMR reflected from vegetation and other features on the ground, and a Remote Cosine Receptor or reference sensor for measuring irradiance or incident radiation measured in watts/m<sup>2</sup> (ASD, Boulder, CO).

Prior to each series of spectral measurements and at frequent intervals thereafter, a white reference measurement was obtained using a Spectralon<sup>®</sup> refer-

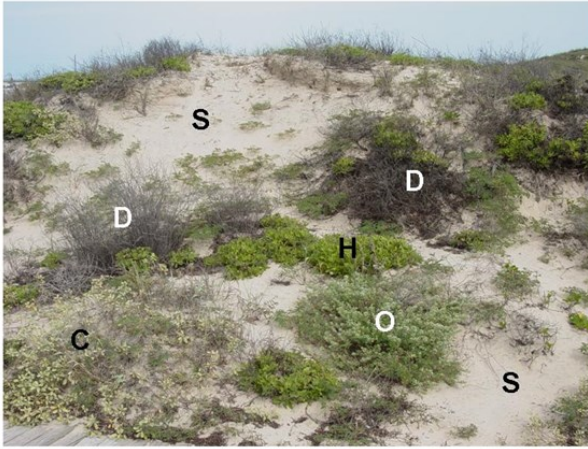


**Fig. 2.** Major landscape features of the research areas on South Padre Island included a mixture of live vegetation such as camphor weed (H), beach evening primrose (O), and beach croton (C), residue of dead vegetation (D) and sand (S). These particular plant species appear to be distinguishable in the visible region of the spectrum, and all are highly distinct from dead vegetation and sand.

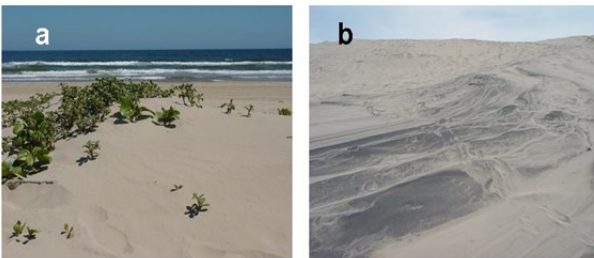


**Fig. 3.** Typical beach sand occurring on South Padre Island (a) and deposits of magnetite that are commonly evident within dune areas during certain periods of the year (b).

ence panel (ASD, Boulder, CO) to facilitate the real-time conversion of radiance measurements to values representing percent reflectance in situ using RS<sup>3</sup> Dual<sup>®</sup> software (Analytical Spectral Devices, Boulder, CO). The instantaneous field of view (IFOV) of the target sensor was constrained by use of an 18° IFOV adapter, and the sensor was normally held at a distance of 0.5 – 1.0 m above the target at the time of measurement. A minimum of 5 spectral measurements were obtained for each type of target on each sampling occasion. Spectral measurements were processed using ViewSpec Pro<sup>®</sup> software (ASD, Boulder, CO), and estimates of percent reflectance at selected wavelengths in the green, red and NIR regions (550, 650 and 850 nm, respectively) for each replicate were subjected to one-way analysis of variance (ANOVA) and

the Tukey HSD test for ad hoc comparisons included in SYSTAT 10 (SPSS, Inc., Chicago, IL).

**Aerial Surveys.** Aerial surveys of the three research sites were conducted by personnel of the USDA Agricultural Research Service on five occasions (June, 2003; February and June, 2004; February and June, 2005) using either of two aircraft platforms - a single-engine Cessna 206 and a twin-engine Cessna 404 Titan, both of which were equipped with camera ports (Figure 4a). In all surveys, exposures were made on Kodak Aerochrome 1443 (23 x 23 cm) CIR film using a Fairchild KA-2 camera (Figure 4b) equipped with a 12-in focal length lens and appropriate filters (Wratten 15 and CC10). Surveys of each site were conducted at two altitudes (2,500 and 5,000 ft) during the mid-afternoon period (1400 – 1500 hrs) under clear sunny conditions, and included a minimum of three sequential frames at each altitude with 60% endlap to provide stereoscopic coverage of the target area (this was required for a related objective of the project). In order to facilitate the geometric correction (rectification) of aerial CIR photographs, 20 - 30 black plastic targets, each measuring approximately 1.0 × 1.0 m, were installed in a systematic pattern within each site on the morning of each scheduled survey (Figure 5a), and three-dimensional coordinates (latitude, longitude and elevation) of the center of each target was measured using survey-grade GPS equipment (Figure 5b).



**Fig. 4.** Aircraft platforms and camera system used in aerial surveys of South Padre Island research sites: single-engine Cessna 206 and twin-engine Cessna 404 Titan (a) and Fairchild KA-2 camera with 12-in focal length lens (b) mounted in aircraft (courtesy of Agricultural Research Service, U. S. Department of Agriculture).

**Image Processing.** Because of the fact that native vegetation within dune zones on South Padre Island typically occur in small patches separated by variable-sized patches of sand (Figure 4), we considered it essential to utilize imagery with high spatial resolution for development of image classifications. CIR film acquired in each aerial survey was therefore processed and scanned at a resolution of 1,200 dpi (21.7 mi-

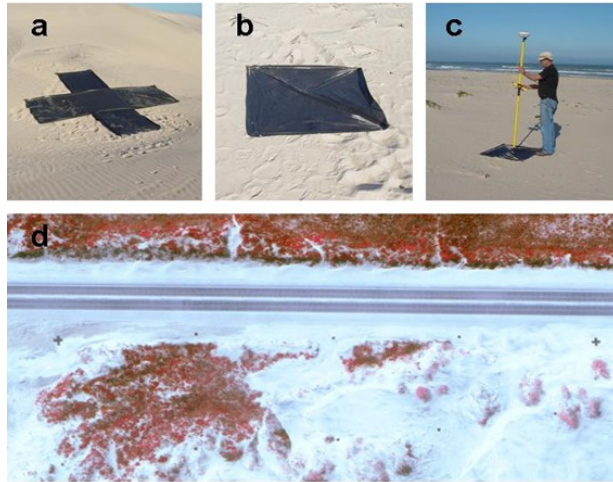


**Fig. 5.** Black plastic ground targets placed within each site on the day of each aerial survey included x-shaped end markers (a) and square targets (b). Precise 3-dimensional coordinates of the center of each target were measured using survey-grade GPS equipment (c). Targets were clearly visible in an aerial CIR photograph of Site 2 acquired at an altitude of 5,000 ft (d) and were used in all surveys for georeferencing of imagery and extraction of digital elevation models using photogrammetric techniques.

crons) using an Epson Expression® 1600 tabletop scanner (Epson America, Inc., Long Beach, CA). This scanning resolution provided image ground pixel resolutions which approached the resolving power of the film itself (e.g., 0.05m at scale of 1:2,500 and 0.12m at 1:5,000 scale). Digitized CIR imagery was imported into Idrisi Kilimanjaro® (Clark University, Worcester, MA) and georeferenced to a standard coordinate system (NAD83 UTM Zone 14N). Images were resampled to a resolution of 0.1 m using the *nearest neighbor* technique, which does not alter original brightness values of imagery (Jensen 2005).

Quality assessments of georeferenced imagery were based evaluation of the *root mean square error* (RMSE), which is calculated as follows:  $RMSE = [ (r - x)^2 + (c - y)^2 ]^{1/2}$  where *r* and *c* represent the transformed row and columns of individual Ground Control Points (GCPs) within the raw image, respectively, and *x* and *y* represent the true geographic coordinates of these same points (Wilke and Finn 1996). When summed over all points, the RMSE provides an assessment of total error involved in the translation of image pixel locations to true geographic coordinates (Wilke and Finn 1996). Because of the accuracy required by this project, efforts were made to maintain RMSE within a range of 1-2 pixels (equivalent to 0.12 - 0.24 m ground resolution).

**Image Classifications and Accuracy Assessments.** Thematic vegetation maps were developed from rectified imagery (green, red and NIR waveband images of CIR photographs) using supervised image classifications based on a maximum likelihood procedure (Clark Labs 1999). “Training areas” comprised of samples of pixels with known identity (e.g., live and dead vegetation, bare sand and water) were delineated using a combination of on-screen digitizing and overlays of “area features” recorded *in situ* using mapping-grade GPS equipped with real-time differential correction (Omnistar® Furgo Consultants, Houston, TX) which provides accuracy in the sub-meter range. The bounding rectangle for each image classification was defined as the area encompassed by the ground targets (see previous discussion), and spectral categories were pooled into three broad information classes – vegetative cover (i.e., the aggregate of live and dead vegetation of all species), bare sand (dry and wet areas, including those with dark magnetite deposits) and water (Figures 6 - 8).

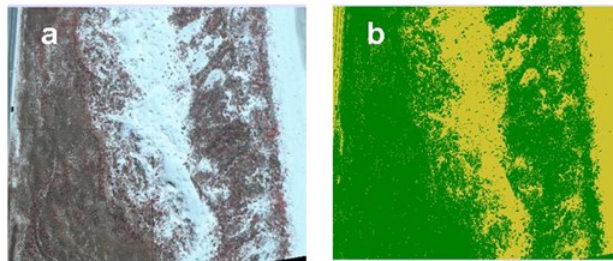


**Fig. 6.** Comparison of aerial CIR photographs (a) and thematic vegetation maps (b) of Site 1 for February, 2004.

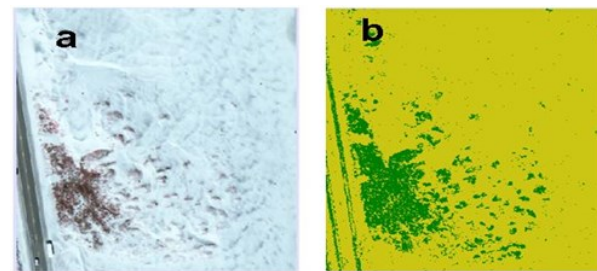


**Fig. 7.** Comparison of aerial CIR photographs (a) and thematic vegetation maps (b) of Site 2 for February, 2004.

Accuracy assessments of thematic maps were based on analysis of *error* or *confusion* matrices, which summarize correct and incorrect assignment of pixels to categories included in the image classification (Congalton and Green 1999). *Overall accuracy* of a given classification was calculated as total num-

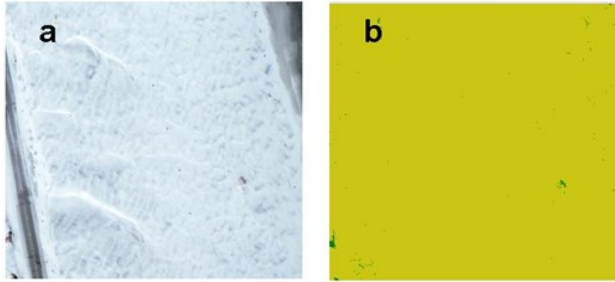


**Fig. 8.** Comparison of aerial CIR photographs (a) and thematic vegetation maps (b) of Site 3 for February, 2004.

bers of pixels along the diagonal of the matrix (i.e., those correctly classified in all categories) as a percentage of the total number of pixels included in the classification. *Producer's accuracy*, which represents the number of pixels for a given category (within a given column) which are classified correctly, was calculated as total number of pixels in the diagonal of that particular column as a percentage of the column total for that particular category. *User's accuracy*, which represents the total number of classified pixels of a given category which were correctly classified as such, was calculated as the total number of pixels along the diagonal of a particular row by the row total for that category. Comparison of producer's and user's accuracies for each category in the classification to evaluate the degree to which various categories were confused, either by errors of omission (define) or errors of commission (define). The *Kappa* statistic ( $K$ ), defined as

$$K = \frac{N \sum_{i=1}^r x_{ii} - \sum_{i=1}^r (x_{i+} \cdot x_{+i})}{N^2 - \sum_{i=1}^r (x_{i+} \cdot x_{+i})}$$

where  $r$  = number of rows in matrix,  $x_{ii}$  = number of observations in row  $i$  and column  $i$  (along main diagonal),  $x_{i+}$  = number of observations in row  $i$ ,  $x_{+i}$  = number of observations in column  $i$ , and  $N$  = number of observations in matrix, was used to compare the accuracy of a given classifier to that which would have been obtained using a random classifier (Lillesand et al. 2004).

**Change-Detection Analyses.** Thematic vegetation maps developed from CIR imagery acquired during each aerial survey were used to estimate the areal extent of vegetative cover occurring within each study site of the three research sites, and to evaluate the spatial distribution of changes occurring within each site during each time six-month interval. In the first case, binary masks were created by assigning a category

value of '1' to vegetative cover and a value of '0' to sand or water, and measuring the total area of category '1' using an area-measurement algorithm (Clark Labs 1999). In the second case, thematic maps for comparable time periods (February, 2004 and February, 2005; June, 2004 and June, 2005) were compared on a pixel-by-pixel basis using a cross-tabulation procedure (Clark Labs 1999) and images were developed showing locations of vegetative losses (a given pixel was classified as vegetative cover at time  $t$  and as sand at time  $t+1$ ), vegetative gains (pixel classified as sand at time  $t$  and as vegetative cover at time  $t+1$ ) and areas of no change (no change in pixel during time interval). A principal advantage of this type of change-detection analysis is that it not only provides information regarding the magnitude of change during a given time interval, but also provides an image (map) showing the spatial distribution of various changes within the study area (Lunetta and Elvidge 1999).

## RESULTS AND DISCUSSION

**Spectral Reflectance Measurements.** Representative plant species occurring in dune fields exhibited spectral profiles typical of those for healthy foliage in general, i.e., relatively low reflectance in the blue and red regions of the spectrum, slightly higher reflectance in the green region, and a substantial increase in reflectance of near-infrared wavelengths (Figure 9a). The relatively low reflectance of blue and red wavelengths is primarily an effect of absorption by photosynthetic pigments (particularly chlorophylla) while the pronounced increase of near-infrared reflectance is primarily an effect of leaf structure, i.e., the configuration and condition of air spaces in the spongy mesophyll layer of leaves (Gausman 1985). In contrast, spectral profiles for dead vegetation (stalks and residue on soil surface) were basically similar in shape to those for sand and dark magnetite deposits, i.e., a progressive increase in reflectance with increases in wavelength (Figure 9b). In terms of magnitude, however, reflectance of visible and near-infrared wavelengths was greatest for sand, intermediate for dark magnetite deposits, and least for dead vegetation, stalks and residue. Thus, each of these landscape features (live vegetation, dead vegetative cover, and sand, including areas with magnetite deposits) appear to be spectrally distinct in one or more waveband regions during all seasonal periods, which is requisite for detection in broadband CIR imagery and for their use as meaningful information categories in automated image classifications (Figure 10).

CIR aerial photographs acquired on each of four survey dates were digitized and georeferenced to a standard coordinate system (NAD83 UTM Zone 14N).

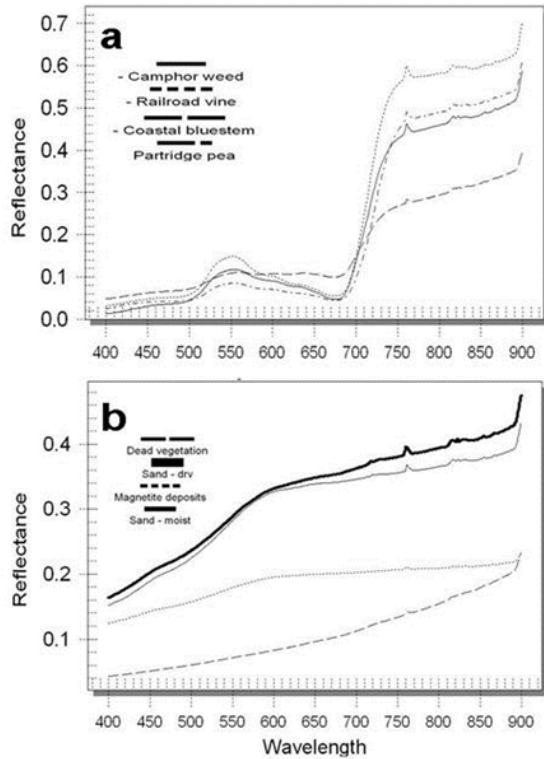


**Fig. 9.** Spectral profiles for representative native plant species (a) and sand, magnetite deposits, and dead vegetation (b) within dune fields of South Padre Island, Texas (2004).

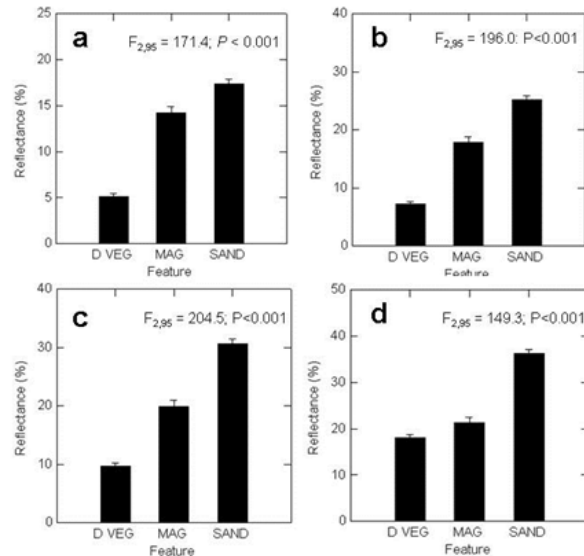


**Fig. 10.** Comparison of spectral reflectance by dead vegetation (DVEG), magnetite deposits (MAG) and dry sand (SAND) in the blue region at 480 nm (a), in the green region at 550 nm (b), in the red region at 680 nm (c) and in the NIR region at 880 nm (d).

In all cases, a linear (first-degree polynomial) transformation was sufficient to provide an acceptable level of geometric correction, with root mean square errors (RMSEs) ranging between 0.987 – 1.496 for Site 1, 0.397 – 2.501 for Site 2, and 0.712 – 2.867 for Site 3 (Table 1).

The correspondence between aerial CIR photographs and thematic vegetation maps developed from such imagery was remarkably consistent on all four

**Table 1.** Metadata for rectified and georeferenced CIR photographs acquired in aerial surveys of South Padre Island during 2004-2005 (NAD83 UTM Zone 14N).

Date of Acquisition	Site	Ground Pixel Resolution (m)	Transformation	RMSE
Feb 2004	1	0.12	Linear	0.987
	2			0.575
	3			0.712
June 2004	1	0.12	Linear	1.085
	2			0.397
	3			0.788
Feb 2005	1	0.12	Linear	0.988
	2			2.501
	3			2.867
June 2005	1	0.12	Linear	1.496
	2			1.231
	3			1.013

survey occasions (Figures 6 - 8). Overall accuracy of supervised image classifications for the two vegetated

**Table 2.** Accuracy assessment of thematic vegetation maps developed from CIR imagery acquired on South Padre Island, Texas, 2004-2005.

Date of Acquisition	Site	Accuracy (%) <sup>a</sup>			Kappa
		Producer's	User's	Overall	
Feb 2004	1	89.8	96.3	91.9	0.8349
	2	83.3	71.4	93.9	0.7346
June 2004	1	95.7	95.7	94.0	0.8571
	2	90.9	90.9	96.0	0.8834
Feb 2005	1	96.7	96.7	90.9	0.8267
	2	75.0	100.0	98.0	0.8466
June 2005	1	90.7	100.7	92.9	0.8249
	2	90.3	93.3	94.9	0.8816

<sup>a</sup> Based on analysis of pixels classified as total (live and dead) vegetative cover.

areas (Sites 1 and 2) ranged between 90.9 – 94.0% for the former and 93.9 – 98.0% for the latter (Table 2).

*Producer's accuracy* for vegetative cover, indicative of the percentage of pixels that were correctly classified as vegetative cover, ranged between 89.8 – 96.7 for Site 1 and 75.0 – 90.9% for Site 2. *User's accuracy*, indicative of vegetative cover in the field

that was correctly classified as such, ranged between 96.3-100% for Site 1 and 71.4 – 100% for Site 2. The magnitude of the *Kappa* coefficients suggested that the image classifications for Site 1 were 82.5 – 85.7% better than levels that would have been achieved by use of a random classifier, and those for Site 2 were 73.5 – 84.6% better than would have been attained by random assignment of pixels (Table 2). These consistently high levels of thematic accuracy were primarily attributable to the use of a few relatively simple (but meaningful) information classes comprised of features which were spectrally distinct in one or more wave-band regions during all seasonal periods.

As many of the native plant species inhabiting the South Padre Island dune systems are annuals (e.g., partridge pea, *Chamaecrista fasciculata*) while others are perennials (e.g., camphor weed, *Heterotheca subaxilaris*), vegetation change-detection analyses for each site were based on comparable time periods, i.e., February, 2004 – February, 2005 and June, 2004 – June, 2005. In the first comparison, vegetative cover appears to have decreased slightly from 65.6% to

**Table 3.** Estimated changes in total vegetative cover within Sites 1 and 2 during two 12-month comparison periods (2004-2005).

Site	Period	Vegetative Cover (m <sup>2</sup> )	% of Area Covered <sup>a</sup>	Δ Change (%)
1	Feb, 2004	39,339	65.6	
	Feb, 2005	38,238	63.8	-1.8
	June, 2004	43,907	73.2	
	June, 2005	38,868	64.8	-8.4
2	Feb, 2004	3,458	13.4	
	Feb, 2005	2,716	10.5	-2.9
	June, 2004	5,394	20.9	
	June, 2005	5,963	23.1	2.2

<sup>a</sup> Based on an estimated area of 59,964 m<sup>2</sup> within the map for Site 1 and 25,799 m<sup>2</sup> within the map for Site 2.

63.8% ( $\Delta = -1.8\%$ ) in Site 1 and from 13.4% to 10.5% ( $\Delta = -2.9\%$ ) in Site 2 (Table 3).

Most of the apparent changes within Site 1 appear to have involved small areas that were concentrated along sand – vegetation boundaries which delineated the major topographic zones of the dune system (Figures 11 and 12).

A similar pattern was evident within Site 2, except that apparent gains and losses of vegetative cover involved larger areas, including one which was clearly the result of human activities (discussion to follow).

In the second comparison (June, 2004 – June, 2005), vegetative cover decreased from 73.2% to 64.8% ( $\Delta = -8.4\%$ ) in Site 1 but increased slightly from 20.9% to 23.1% ( $\Delta = 2.2\%$ ) in Site 2 (Table 3).

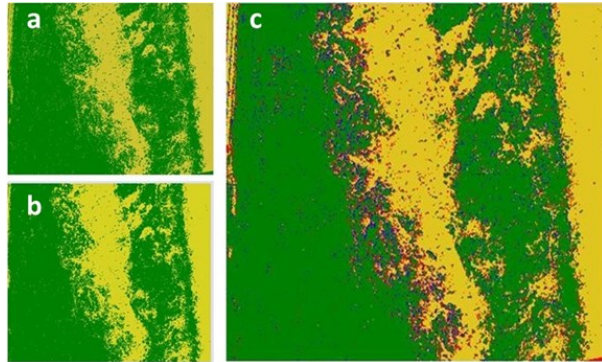


**Fig. 11.** Supervised image classifications of Site 1 for February, 2004 (a) and February, 2005 (b) and resulting change-detection map (c) showing areas of “no change” (light yellow), apparent losses (red) and apparent gains (blue) in total vegetative cover.

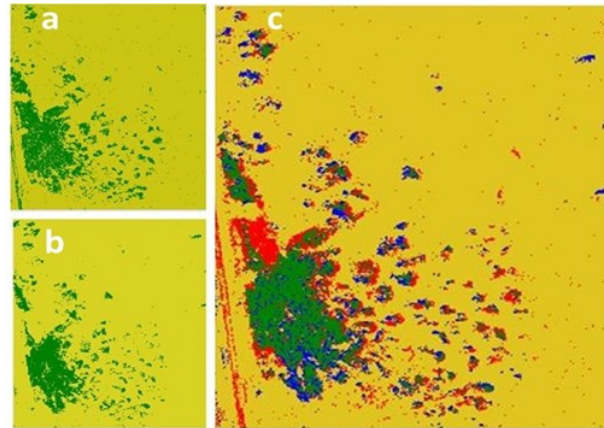


**Fig. 12.** Supervised image classifications of Site 2 for February, 2004 (a) and February, 2005 (b) and resulting change-detection map (c) showing areas of “no change” (light yellow), apparent losses (red) and apparent gains (blue) in total vegetative cover.

A change-detection map for Site 1 detected an appreciable increase in apparent vegetation losses which appears to have been largely concentrated in the back-shore zone and along the gentle slope (west face) of the primary dune (Figure 13c). In contrast, apparent vegetative gains were evident in most areas of Site 2, with the exception of a relatively large area located near the site of the disruption noted in the first comparison (Figure 14c).

As indicated previously, the series of aerial CIR photographs acquired at Site 2 between June, 2004 and June, 2005 detected a significant perturbation which was caused by the dumping of sand by highway maintenance personnel during late-2004. The sequence

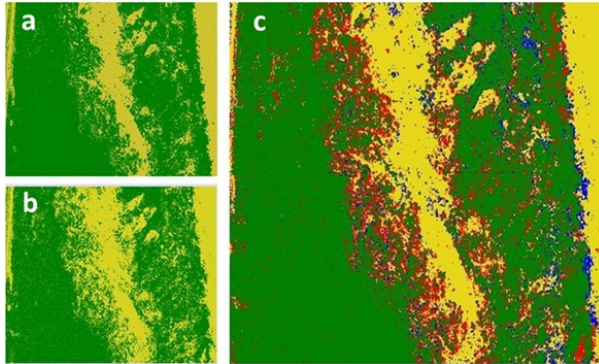


**Fig. 13.** Supervised image classifications of Site 1 for June, 2004 (a) and June, 2005 (b) and resulting change-detection map (c) showing areas of “no change” (light yellow), apparent losses (red) and apparent gains (blue) in total vegetative cover.

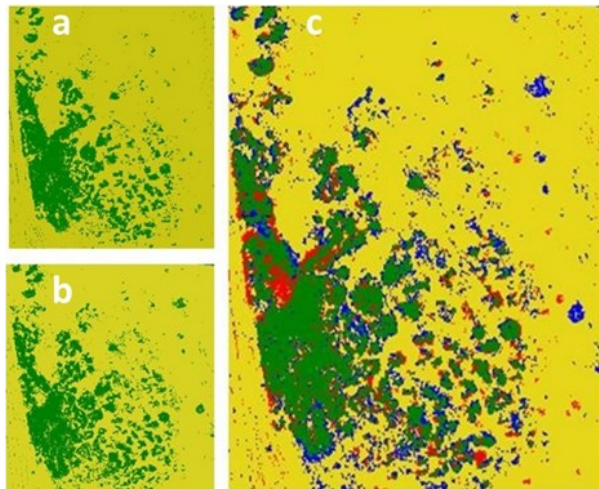


**Fig. 14.** Supervised image classifications of Site 2 for June, 2004 (a) and June, 2005 (b) and resulting change-detection map (c) showing areas of “no change” (light yellow), apparent losses (red) and apparent gains (blue) in total vegetative cover.

of CIR photographs clearly shows the original extent of vegetative cover at the site (Figure 15a), the area disrupted by the sand-dumping incident (Figure 15b) and the extent of recolonization by native plant species, particularly railroad vine, *Ipomoea pes-capae*, approximately six months later (Figure 15c).

The seasonal estimates of vegetative cover obtained from thematic vegetation maps were remarkably close those obtained using the conventional line transect method of sampling which indicated 57% vegetative cover at Site 1 and 12.5% at Site 2 (Judd et al. 2008). Although the two methods are different,

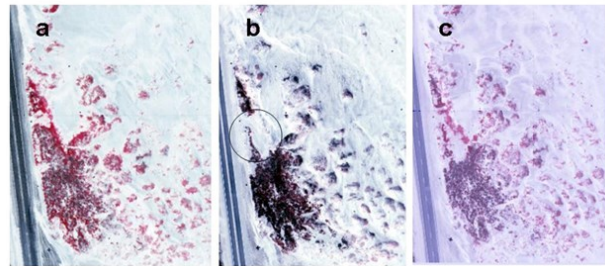


**Fig. 15.** Aerial CIR photographs of Site 2 taken during June, 2004 (a), indicating a disruption in native vegetation caused by sand dumping (see encircled area in b), and partial recovery of native vegetation by June, 2005 (c).

both indicated that changes in vegetative cover at the two sites had been minimal during the course of the study. However, a significant (but localized and temporary) reduction in vegetation cover at Site 2, which was caused by the dumping of sand by highway maintenance crews during late-2004, was clearly evident in a series of aerial CIR photographs acquired before and after the sand-dumping incident (Figure 15a,b). This particular situation exemplifies one of the principal advantages of remote sensing technology relative to other survey methodologies used in coastal research, i.e., aerial CIR photographs provided the means by which to evaluate not only the location and extent of the original disturbance, but also its eventual recovery as a result of recolonization by native plant species, particularly railroad vine, *Ipomoea pes-capae* (Figure 15c).

## CONCLUSIONS

Change-detection analyses based on temporal comparisons of high-resolution image classifications derived from aerial CIR photographs were consistent with interpretations based on conventional line-transect sampling methods. Both procedures indicated that temporal changes in vegetation patterns within three research sites had been minimal during the course of the 2-year study. However, both procedures detected a significant but localized disruption of native vegetation caused by sand-dumping by highway maintenance crews during late-2004, and the former (aerial photographs) documented the extent of the disturbance and the eventual recolonization of the disturbance by native vegetation during the following year. By providing a “bird’s eye” view of the environment, aerial CIR imagery and other forms of remotely sensed imagery provide resource managers with relatively inexpensive and powerful methodologies for



monitoring and quantifying events that would be difficult to achieve by other means.

### ACKNOWLEDGMENTS

We are grateful to the National Oceanic and Atmospheric Administration, the Coastal Coordination Council of the Texas General Land Office (GLO Contract # 04-007), Austin, Texas, and the University of Texas Rio Grande Valley (formerly the University of Texas – Pan American) for financial support during the course of this study.

### LITERATURE CITED

- Campbell, J. B. 2007. Introduction to Remote Sensing (4th ed). Guilford, NY.
- Clark Labs. 1999. Guide to GIS and Image Processing – Volume 2. Clark University, Worcester, MA.
- Congalton, R. G. and K. Green. 1999. Assessing the Accuracy of Remotely Sensed Data: Principles and Practices. Lewis Publishers, Boca Raton, FL.
- Everitt, J. H., and F. W. Judd. 1989. Using Remote Sensing Techniques to Distinguish and Monitor Black Mangrove (*Avicennia germinans*). Journal of Coastal Research. 5(4):737-745.
- Everitt, J. H., D. E. Escobar, and F. W. Judd. 1991. Evaluation of Airborne Video Imagery for Distinguishing Black Mangrove (*Avicennia germinans*) on the Lower Texas Gulf Coast. Journal of Coastal Research. 7: 1169-1173.
- Everitt, J. H., F. W. Judd, D. E. Escobar, and M. R. Davis. 1996. Integration of Remote Sensing and Spatial Information Technologies for Mapping Black Mangrove on the Texas Gulf Coast. Journal of Coastal Research. 12(1): 64-69.
- Everitt, J. H., C. Yang, K. R. Summy, F. W. Judd, and M. R. Davis. 2007. Evaluation of Color-Infrared Photography and Digital Imagery to Map Black Mangrove on the Texas Gulf Coast. J. Coastal Research 23(1):230-235.
- Everitt, J. H., C. Yang, S. Sriharan, and F. W. Judd. 2008. Using high-resolution satellite to map black mangrove on the Texas Gulf Coast. Journal of Coastal Research 24(6):1582-1586.
- Gausman, H. W. 1985. Plant leaf optical properties in visible and near-infrared light. Graduate Studies No. 29, Texas Tech University. Texas Tech Press, Lubbock, TX. 79 pp.
- Jensen, J. R. 2005. Introductory Digital Image Processing: A Remote Sensing Perspective. Prentice Hall, Upper Saddle River, NJ.
- Judd, F. W., and S. L. Sides. 1983. The impact of Hurricane Allen on the near-shore vegetation of South Padre Island. Southwestern Naturalist 28:365-369.
- Judd, F. W., R. I. Lonard, and S. L. Sides. 1977. The vegetation of South Padre Island, Texas in relation to topography. Southwestern Naturalist 22 (1):31-48.
- Judd, F. W., R. I. Lonard, K. R. Summy, and R. A. Mazariegos. 2007. Seasonal variation in dune vegetation at South Padre Island, Texas. Texas J. Sci. 59:113-126.
- Judd, F. W., K. R. Summy, R. I. Lonard, and R. Mazariegos. 2008. Dune and vegetation stability at South Padre Island, Texas, United States of America. J. Coastal Research 24:992-998.
- Lillesand, T. M., R. W. Kiefer, and J. W. Chipman. 2004. Remote Sensing and Image Interpretation. John Wiley and Sons, New York.
- Lonard, R. I., and F. W. Judd. 1980. Phytogeography of South Padre Island, Texas. The Southwestern Naturalist 25:313-322.
- Lonard, R. I., and F. W. Judd. 1981. The terrestrial flora of South Padre Island, Texas. Austin (TX): University of Texas at Austin. Miscellaneous papers, Texas Memorial Museum. 74 pp.
- Lonard, R. I. and F. W. Judd. 1985. Effects of a Severe Freeze on Native Woody Plants in the Lower Rio Grande Valley, Texas. The Southwestern Naturalist. 30(3): 397-403.
- Lonard, R. I., F. W. Judd, J. H. Everitt, and D. E. Escobar. 1991. Roadside associated disturbance on coastal dunes. Pp. 2823-2836 in: Proceedings Seventh Symposium on Coastal and Ocean Management, "Coastal Zone '91". Am. Soc. of Civil Engineers. Long Beach, California.
- Lonard, R. I., and F. W. Judd. 1993. Recovery of vegetation of barrier island washover zones, pp. 2324-2331 In Proc. Eighth Symp. On Coastal and Ocean Management, "Coastal Zone '93". American Soc. Civil Engineers, New Orleans, LA, 3512 pp.
- Lonard, R. I., and F. W. Judd. 1997. The biological flora of coastal dunes and wetlands. *Sesuvium portulacastrum*. J. Coastal Research 13:96-104.
- Lonard, R. I., F. W. Judd, and S. L. Sides. 1978. Annotated Checklist of the Flowering Plants of South Padre Island, Texas. The Southwestern Naturalist. 23:497-510.
- Lonard, R. I., F. W. Judd, J. H. Everitt, D. E. Escobar, M. A. Alaniz, I. Cavazos III, and M. R. Davis. 1999. Vegetative change on South Padre Is-

- land, Texas, over twenty years and evaluation of multispectral videography in determining vegetative cover and species identity. *Southwestern Naturalist* 44:261-271.
- Lunetta, R. S., and C. D. Elvidge. 1999. *Remote Sensing Change Detection: Environmental Monitoring Methods and Applications*. Taylor and Francis, London.
- Mazariegos, R. A., K. R. Summy, F. W. Judd, R. I. Lonard, M. R. Heep, J. H. Everitt, and M. R. Davis. 2005. Evaluation of CIR Photography in the Development of Vegetation Maps for Spoil Islands of the Lower Laguna Madre, Texas. 20<sup>th</sup> Biennial Workshop on Aerial Photography, Videography, and High Resolution Digital Imagery for Resource Assessment 05': 1-7.
- Richardson, A. 2002. *Wildflowers and Other Plants of Texas Beaches and Islands*. University of Texas Press: Austin, TX.
- Summy, K. R., F. W. Judd, R. I. Lonard, and R. A. Mazariegos. 2005a. "Relationship Between Native Vegetative Cover and Stability of Dune Systems Occurring on South Padre Island, Texas." Final Report of Coastal Management Program Project (GLO 04-007) - Submitted to Coastal Management Program, Texas General Land Office, Austin, TX, August 29, 2005.
- Summy, K. R., F. W. Judd, R. I. Lonard, R. A. Mazariegos, J. H. Everitt, and M. R. Davis. 2005b. Effectiveness of Aerial Color Infrared Photography for Mapping Vegetative Cover Within Dune Areas of South Padre Island, Texas. 20<sup>th</sup> Biennial Workshop on Aerial Photography, Videography, and High Resolution Digital Imagery for Resource Assessment 05': 1-12.
- Wilke, D. S., and J. T. Finn. 1996. *Remote Sensing Imagery for Natural Resources Monitoring*. Columbia University Press, New York.